CHEMISTRY
A EUROPEAN JOURNAL

DOI: 10.1002/chem.200901673

Photochemical Reduction of Carbon Dioxide Catalyzed by a Ruthenium-Substituted Polyoxometalate

Alexander M. Khenkin,[a] Irena Efremenko,[a] Lev Weiner,[b] Jan M. L. Martin,[a] and Ronny Neumann*[a]

Abstract: A polyoxometalate of the Keggin structure substituted with Ru^{III}, $^{6}Q_5[Ru^{III}(H_2O)SiW_{11}O_{39}]$ in which $^{6}Q = (C_6H_{13})_4N^+$, catalyzed the photoreduction of CO_2 to CO with tertiary amines, preferentially Et_3N, as reducing agents. A study of the coordination of CO_2 to $^{6}Q_5[Ru^{III}(H_2O)SiW_{11}O_{39}]$ showed that 1) upon addition of CO_2 the UV/Vis spectrum changed, 2) a rhombic signal was obtained in the EPR spectrum ($g_x = 2.146$, $g_y = 2.100$, and $g_z = 1.935$), and 3) the ^{13}C NMR spectrum had a broadened peak of bound CO_2 at 105.78 ppm ($\Delta_{1/2} = 122$ Hz). It was concluded that CO_2 coordinates to the Ru^{III} active site in both the presence and absence of Et_3N to yield $^{6}Q_5[Ru^{III}(CO_2)SiW_{11}O_{39}]$. Electrochemical measurements showed the reduction of Ru^{III} to Ru^{II} in $^{6}Q_5[Ru^{III}(CO_2)SiW_{11}O_{39}]$ at -0.31 V versus SCE, but no such reduction was observed for $^{6}Q_5[Ru^{III}(H_2O)SiW_{11}O_{39}]$. DFT-calculated geometries optimized at the M06/PC1//PBE/AUG-PC1//PBE/PC1-DF level of theory showed that CO_2 is preferably coordinated in a side-on manner to Ru^{III} in the polyoxometalate through formation of a Ru–O bond, further stabilized by the interaction of the electrophilic carbon atom of CO_2 to an oxygen atom of the polyoxometalate. The end-on CO_2 bonding to Ru^{III} is energetically less favorable but CO_2 is considerably bent, thus favoring nucleophilic attack at the carbon atom and thereby stabilizing the carbon sp^2 hybridization state. Formation of a O_2C–NMe_3 zwitterion, in turn, causes bending of CO_2 and enhances the carbon sp^2 hybridization. The synergetic effect of these two interactions stabilizes both Ru–O and C–N interactions and probably determines the promotional effect of an amine on the activation of CO_2 by $[Ru^{III}(H_2O)SiW_{11}O_{39}]^{5-}$. Electronic structure analysis showed that the polyoxometalate takes part in the activation of both CO_2 and Et_3N. A mechanistic pathway for photoreduction of CO_2 is suggested based on the experimental and computed results.

Keywords: carbon dioxide · photochemistry · polyoxometalates · reduction · ruthenium

Introduction

The rise in the amount of CO_2 in the atmosphere and its deleterious climatic effects together with a desire to reduce our dependence on fossil fuels have made the objective of a carbon-neutral energy platform a very important one. Three major directions have been described: nuclear energy, carbon capture by CO_2 sequestration and storage, and renewable energy.[1] In the renewable energy sector, solar energy is the most abundant source. Concepts related to chemical (not photovoltaic or biological) storage of solar energy reveal that artificial photosynthesis continues to be a captivating idea as well as the related splitting of water to H_2 and O_2 by using various approaches.[2] We are interested in exploring the use of CO_2 as a chemical energy source. In the past, aspects of CO_2 utilization have typically been discussed in terms of hydrogenation and reactivity with nucleophiles, such as amines and epoxides.[3] Several other concepts have been put forth for the transformation of CO_2 to CO which include 1) reductive cleavage and related disproportionation reactions,[4] 2) photoreduction with H_2O by semiconductors such as TiO_2,[5] and 3) photocatalytic reduction that has been carried out in the presence of sacrificial

[a] Dr. A. M. Khenkin, Dr. I. Efremenko, Prof. J. M. L. Martin, Prof. R. Neumann
Department of Organic Chemistry
Weizmann Institute of Science
Rehovot 76100 (Israel)
Fax: (+972) 8-9344142
E-mail: Ronny.Neumann@weizmann.ac.il

[b] Dr. L. Weiner
Chemical Research Support Unit
Weizmann Institute of Science
Rehovot 76100 (Israel)

Supporting information for this article is available on the WWW under http://dx.doi.org/10.1002/chem.200901673.

reducing agents, typically trialkylamines and trialkanolamines.[6–9] In the last area a wide range of transition-metal coordination compounds based on iron,[6] cobalt,[7] ruthenium,[8] and rhenium[9] have been suggested as photocatalysts; often a photosensitizer is also needed. Given the potential sensitivity of transition-metal coordination compounds to photodegradation, there is an inherent interest in examining the photoreduction of CO_2 with an inorganic photocatalyst such as a polyoxometalate. Although oxidative photochemistry mediated by polyoxometalates has been intensively studied,[10] there have been no reliable reports on the photoreduction of CO_2 catalyzed by polyoxometalates. There have, however, been several reports of polyoxometalates binding or coordinating CO_2,[11] and some reports on the use of polyoxometalates in the related electrochemical and photochemical oxidation of water to O_2.[12] By the use of a combined experimental and computational approach, herein we report on the coordination of CO_2 to a ruthenium-substituted Keggin-type polyoxometalate,[13] and its subsequent photoreduction in the presence of tertiary amines.

Results and Discussion

The coordination of CO_2 to $^6Q_5[Ru^{III}(H_2O)SiW_{11}O_{39}]$, in which ^6Q = tetra-*n*-hexylammonium, was studied in toluene as a noncoordinating solvent, after initial research in coordinating solvents such as acetonitrile revealed no discernible interaction. Similar to previous work on the coordination of O_2 to $^6Q_6[Mn^{II}(H_2O)SiW_{11}O_{39}]$,[14] the bubbling of dry, high-purity CO_2 (99.99%) into a solution of $^6Q_5[Ru^{III}(H_2O)SiW_{11}O_{39}]$ in toluene showed a slight but visible color change from light brown to darker brown. The UV/Vis spectra showed an increase in the optical density at 450 nm and a decrease in optical density at 600 nm, although the spectra with and without the addition of CO_2 are very similar (Figure 1).

The EPR spectrum at 125 K when $^6Q_5[Ru^{III}(H_2O)SiW_{11}O_{39}]$ was purged with Ar (Figure 2, spectrum A) showed peaks at $g = 2.56$ and 2.28. This spectrum is distinct from the EPR spectrum of $^6Q_5[Ru^{III}(H_2O)SiW_{11}O_{39}]$ in 1,2-dichoroethane (without Ar purging) already reported.[15] Upon addition of CO_2 a new spectrum was obtained showing a rhombic signal with g values $g_x = 2.146$, $g_y = 2.100$, and $g_z = 1.935$ (Figure 2, spectrum B). These parameters are similar to those of the ESR spectrum of various octahedral Ru^{III} complexes.[16] The results indicate coordination of CO_2 to the ruthenium-substituted polyoxometalate.

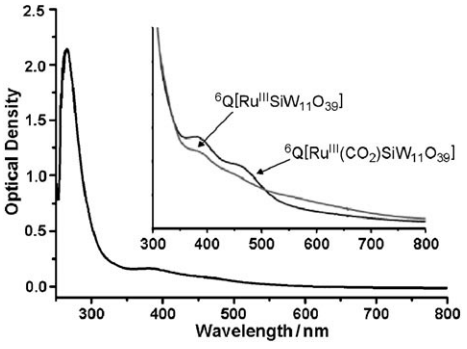

Figure 1. UV/Vis spectrum of a 40 μmol solution of $^6Q_5[Ru^{III}(H_2O)SiW_{11}O_{39}]$ in toluene after purging with Ar ($^6Q_5[Ru^{III}SiW_{11}O_{39}]$) and CO_2 ($^6Q_5[Ru^{III}(CO_2)SiW_{11}O_{39}]$).

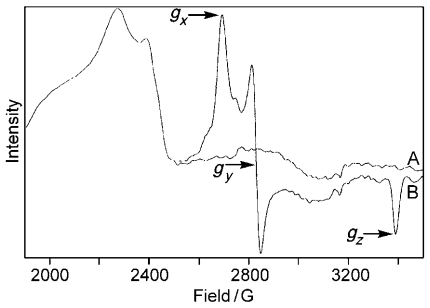

Figure 2. X-band EPR spectra at 125 K of $^6Q_5[Ru^{III}SiW_{11}O_{39}]$ in toluene (A): $g = 2.56$ and 2.28, and $^6Q_5[Ru^{III}(CO_2)SiW_{11}O_{39}]$ in toluene (B): $g_x = 2.146$, $g_y = 2.100$, and $g_z = 1.935$.

Coordinated CO_2 could also be observed by using ^{13}C NMR spectroscopy and ^{13}C-labeled CO_2 (Figure 3). In the ^{13}C NMR spectrum, with short delay times due to the paramagnetic nature of the polyoxometalate, one can observe the coordinated $^{13}CO_2$ shifted up-field to 105.78 ppm ($\Delta_{1/2} = 122$ Hz) relative to noncoordinated CO_2 that appears at 124.48 ppm ($\Delta_{1/2} = 40$ Hz). Use of $^{12}CO_2$ confirmed the assignment of the peak at 105.78 ppm to coordinated CO_2. Importantly, the bubbling of Ar into the solution to replace the CO_2 showed, by the UV/Vis, ESR, and ^{13}C NMR methods, the re-formation of the originally observed spectra. Note that we also attempted to observe the formation of $^6Q_5[Ru^{III}(CO_2)SiW_{11}O_{39}]$ by IR spectroscopy. Such experiments were unsuccessful. Density functional theory (DFT) calculations predicted absorbance at ~1650 cm^{-1} at which there is a peak from the quaternary ammonium cation, thus preventing the observation of the bound CO_2 in this experiment.

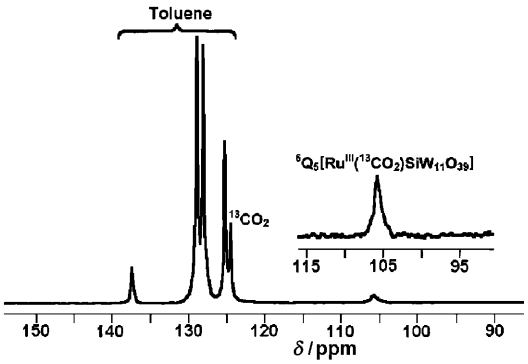

Figure 3. ^{13}C NMR spectrum of $^6Q_5[Ru^{III}(^{13}CO_2)SiW_{11}O_{39}]$.

Therefore, the combined UV/Vis, ESR, and ^{13}C NMR experiments suggest that upon dissolution of $^6Q_5[Ru^{III}(H_2O)SiW_{11}O_{39}]$ (hexacoordinated Ru) in dry toluene, a dehydrated compound, $^6Q_5[Ru^{III}SiW_{11}O_{39}]$ (pentacoordinated Ru), is formed, which after addition of CO_2 yields a CO_2-coordinated compound, formulated as $^6Q_5[Ru^{III}(CO_2)SiW_{11}O_{39}]$ (hexacoordinated Ru; see Equation 1). The coordination of CO_2 was reversible by the addition of Ar, which lowered the CO_2 concentration.

$$^6Q_5[SiRu^{III}(H_2O)W_{11}O_{39}] \underset{}{\overset{PhCH_3}{\rightleftharpoons}} {}^6Q_5[SiRu^{III}W_{11}O_{39}] \overset{CO}{\underset{Ar}{\rightleftharpoons}} {}^6Q_5[SiRu^{III}(CO_2)W_{11}O_{39}] \quad (1)$$

The electrochemical behavior of the ruthenium-substituted polyoxometalate was studied by cyclic voltammetry and was found to be quite different from the reported voltammetric measurement of $[Ru^{III}(H_2O)SiW_{11}O_{39}]^{5-}$ in water.[17] A 1 mM solution of $^6Q_5[Ru^{III}(H_2O)SiW_{11}O_{39}]$ in dichloromethane with 100 mM $(n\text{-butyl})_4N^+BF_4^-$ as electrolyte showed no reduction of the Ru^{III} or W^{VI} of the polyoxometalate (Figure 4a). There is apparently an irreversible oxidation of Ru^{III} to Ru^{IV} at 0.72 V versus SCE. The electrochemical behavior is much changed in the CO_2-bonded compound, $^6Q_5[Ru^{III}(CO_2)SiW_{11}O_{39}]$ (Figure 4b). Here, there appears to be a reversible reduction process at −0.31 V. The peak current was proportional to the square root of the scan rate, although the peak in the reverse scan was not the same size as that observed in the forward scan. Presumably, the peak can be associated with the reduction of Ru^{III} to Ru^{II} that interestingly occurs only in the CO_2-bonded compound. Oxidation reactions that are apparently irreversible were observed at +0.10 and +0.38 V. Upon adding triethylamine (Et_3N), which was used as a proton donor in the photocatalytic study (see below), the cyclic voltammogram was basically unchanged with only a small change in the potential of the second oxidation process (Figure 4c). Similarly, no changes were observed in the EPR and UV/Vis spectra upon addition of Et_3N to $^6Q_5[Ru^{III}(CO_2)SiW_{11}O_{39}]$.

The photochemical reduction of CO_2 was carried out under the following experimental conditions. A Fisher–Porter quartz tube containing 5 mM $^6Q_5[Ru^{III}(H_2O)SiW_{11}O_{39}]$ and 600 mM Et_3N in 3 mL toluene was pressurized with 2 bar CO_2 and pulse-irradiated with a 150 W xenon lamp. In this reaction the amine is used as the electron and proton donor and the polyoxometalate is bifunctional, acting as both the CO_2 complexing agent and photocatalyst.[18] After 20 h, analysis of the reaction mixture by GC revealed the formation of ~50 μmol of CO or about three turnovers based on $^6Q_5[Ru^{III}(H_2O)SiW_{11}O_{39}]$; the quantum yield was ~2%. Carbon monoxide was the only product from CO_2 that was observed: no formic acid, methanol, or methane was detected. In addition, the expected diethylamine and acetaldehyde were also observed.[6–9] It should be recognized that although CO complexes of $[Ru^{III}(H_2O)SiW_{11}O_{39}]^{5-}$ and $[Ru^{II}(H_2O)SiW_{11}O_{39}]^{6-}$ have been reported with expected maxima in the UV/Vis spectrum at 400 and 450 nm, they are not stable when photoirradiated.[19] Significant product inhibition is thus not expected.

As can be seen from Figure 1, the UV/Vis spectrum has a λ_{max} at 259 nm, $\log \varepsilon = 4.73$, which is associated with the oxygen-to-tungsten ligand-to-metal charge-transfer (LMCT) absorption. Commonly used polyoxotungstates, such as $[PW_{12}O_{40}]^{3-}$ and $[W_{10}O_{32}]^{4-}$, are photocatalysts by excitation at the LMCT band,[18] and thus one can assume that here also excitation at the LMCT wavelength can lead to a reactive excited state that is a strong oxidant in this case of triethylamine. Suitably, in the present investigation, excitation at wavelengths longer than 300 nm did not lead to CO_2 reduction, thus

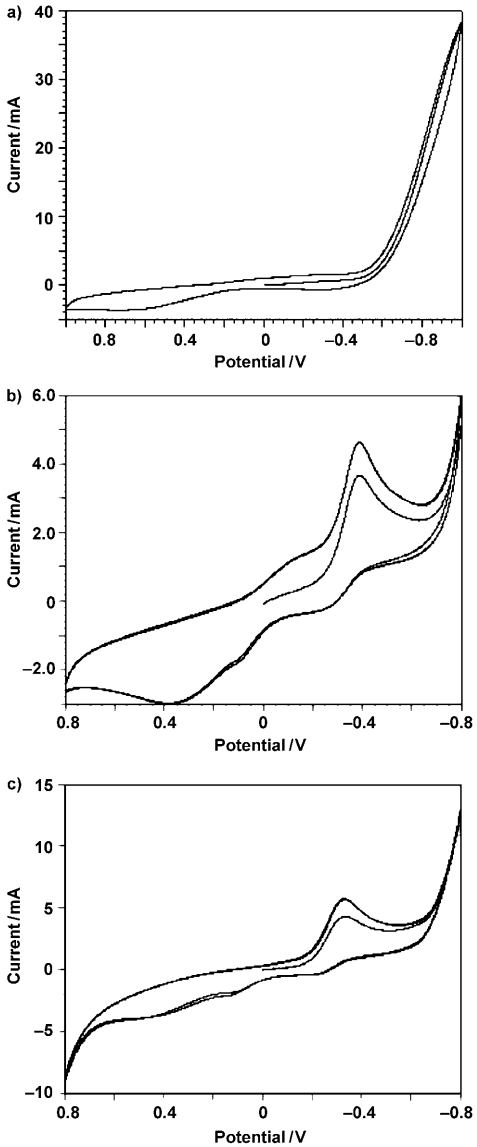

Figure 4. Cyclic voltammetry scans of a) $^6Q_5[Ru^{III}(H_2O)SiW_{11}O_{39}]$, b) $^6Q_5[Ru^{III}(H_2O)SiW_{11}O_{39}]+CO_2$, and c) $^6Q_5[Ru^{III}(H_2O)SiW_{11}O_{39}]+CO_2+Et_3N$. Conditions: 1 mM polyoxometalate, 100 mM $(n\text{-butyl})_4N^+BF_4^-$ in dichloromethane. After the first scan, there was no change in the current–voltage (I–V) plot over 20 scans.

supporting the proposition that excitation at the LMCT band initiates the photoreaction. As is also typical for polyoxotungstates, the excited-state intermediate is not luminescent. Furthermore, control experiments with $[Ru(acac)_3]$ (acac: acetylacetonate) and/or $^6Q_8[SiW_{11}O_{39}]$ did not show the formation of any CO_2 reduction products, which demonstrated the importance of CO_2 coordination to the ruthenium to enable its photochemical reduction. Thus, it indeed appears from the experiments that the ruthenium site of the polyoxometalate coordinates CO_2 and the polyoxometalate "ligand" $[SiW_{11}O_{39}]^{8-}$ acts as a photocatalyst. The stability of the catalyst after photocatalytic experiments was evaluated by IR and UV/Vis spectroscopy; no changes were noticeable relative to the initial spectra, thus indicating that the catalyst was stable.

The use of different amines in the photochemical reduction of CO_2 was probed (Table 1). Triethylamine was the most efficient; diisopropylethylamine showed that the ethyl group is eight times more reactive than the isopropyl group. The use of tribenzylamine showed no formation of CO although the amine was converted. A perfluorinated amine, $(C_4F_9)_3N$, was not reactive because of the lack of a proton source. Interestingly, triphenylamine was also an effective electron and proton donor and formed a nonoxygenated product, *N*-phenylcarbazole.

Table 1. Photochemical reduction of CO_2 with various amines.[a]

Tertiary amine	Converted amine [mol%]	Products	CO [μmol]
Et_3N	12	Et_2NH/CH_3CHO, 1:1	8
Ph_3N	7	*N*-phenylcarbazole	2.8
iPr_2EtN	30	$iPrEtNH+CH_3COCH_3$/ iPr_2NH+CH_3CHO, 1:4	2.4
Bz_3N[b]	79	Bz_2NH, PhCHO, BzN=Bz	0
$(C_4F_9)_3N$	0	–	0

[a] Reaction conditions: 1 mM $^6Q_5[Ru^{III}(H_2O)SiW_{11}O_{39}]$, 50 mM amine in 2 mL toluene, 1 bar CO_2, 20 h of irradiation. [b] Bz: benzoyl.

To gain insight into the geometric and electronic structures of the $[Ru^{III}(CO_2)SiW_{11}O_{39}]^{5-}$ complexes, we undertook a DFT study. Accurate treatment of both strong and weak chemical bonds in such large compounds with a large number of transition-metal atoms is still not straightforward. Our discussion here will be based on the geometries optimized at the PBE/PC1-DF level of theory and electronic energies calculated as $E_e = E[\text{PBE/AUG-PC1-DF}] - E[\text{PBE/PC1-DF}] + E[\text{M06/PC1}]$. Such a combined approach enables calculation of quite accurate energies of the complexes, as is typical for the hybrid meta exchange-correlation functional M06,[20] and allows us to account for the effect of diffuse functions, which is especially important in view of the high negative charge of the model complexes (see the Experimental Section for a further discussion of the choice of the theoretical level). For easy reference, the energies of the interaction of CO_2 with $[Ru^{III}SiW_{11}O_{39}]^{5-}$ (**1**; Figure 5) at several levels of theory are given in Table 2. Key bond lengths optimized by using the PBE/PC1-DF combination (not shown in Figure 5) are summarized in Table 3. A list of energies and bond lengths at other theoretical levels can be found in the Supporting Information. Unless stated otherwise, we will refer to free energies at room temperature (ΔG_{298}).

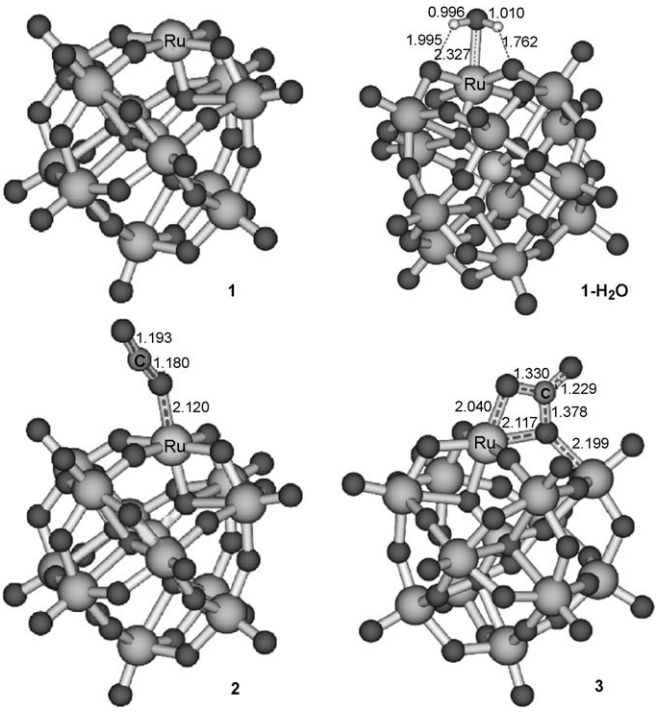

Figure 5. Optimized geometries of polyoxometalate complexes with H_2O and CO_2 (W: large gray spheres, Si: large light gray spheres, O: medium dark gray spheres, H: small white spheres; Ru and C atoms are explicitly labeled). The C–O bond lengths in a free CO_2 molecule optimized at the same theoretical level are 1.176 Å.

Table 2. Calculated energies of interaction of CO_2 and H_2O with polyoxometalate in various complexes [kcal mol^{-1}].

	PBE/PC1-DF ΔE_e	PBE/AUGPC1-DF ΔE_e	M06/PC1 ΔE_e	Combined ΔE_e	Combined ΔG_{298}
1-H_2O	−27.51	−22.22	−28.54	−23.26	−11.44
2	−10.47	−10.25	−9.71	−9.49	−1.13
3	−33.27	−34.31	−36.36	−37.40	−24.03
4-NMe_3[a]	−17.79	−28.32	−18.87	−29.40	−15.39
4-NEt_3[a]	−21.20	−38.32	−21.49	−38.62	−22.53
CO_2–NMe_3[b]	−4.30	−3.15	−6.31	−5.16	4.37
CO_2–NEt_3[b]	−3.97	−12.56	−7.73	−16.34	−7.33

[a] Calculated with respect to free complex **1** and the CO_2–NR_3 (R = Me, Et) adduct. [b] Noncoordinated CO_2–NR_3 complexes are included for comparison.

Our DFT results demonstrated that CO_2 can coordinate with $[Ru^{III}SiW_{11}O_{39}]^{5-}$ (**1**) in end-on and side-on modes resulting in complexes **2** and **3** (see Figure 5). An η^1-C-on coordination was not found because of strong Coulomb repul-

Table 3. Key optimized bond lengths [Å] for various polyoxometalate complexes.

	Si–O_i[a]	Ru–O_i[a]	Ru–O	W–O(Ru)
1	1.694	2.027	1.977, 1.978, 2.021, 2.021	1.855, 1.855, 1.866, 1.866
2	1.687	2.04	2.003, 1.999, 2.006, 2.005	1.845, 1.852, 1.875, 1.876
3	1.679	2.105	1.934, 2.117, 2.050, 2.021	1.840, 2.199, 1.834, 1.846
4-NMe_3	1.686	2.047	2.007, 2.016, 1.999, 2.005	1.845, 1.858, 1.872, 1.873
4-NEt_3	1.685	2.048	2.003, 2.010, 1.997, 2.017	1.841, 1.859, 1.871, 1.875

[a] Subscript "i" is used to denote the inner O atoms involved in the SiO_4 core.

sion between positively charged Ru and C atoms. The side-on coordination mode appears to be energetically the most favorable. Formation of **3** is accompanied by an energy gain of 24.03 kcal mol^{-1} at RT. Natural population analysis (NPA) shows that the CO_2 molecule in **3** keeps a total negative charge of −0.33 whereas the positive charge on the Ru atom decreases from 3.76 in **1** to 3.23 in **3**. Transfer of spin density was not found. The O-C-O bond angle in the coordinated molecule is 126.8°, which indicates an sp^2 hybridization of the carbon atom. Both C–O bonds are elongated with respect to those in a free CO_2 molecule (Figure 5). However, Wiberg bond indexes (WBIs) indicate that the C–O bond directly involved in the interaction with **1** could be considered as a single bond (WBI = 1.13 with respect to 1.90 in free CO_2), whereas the dangling C–O bond preserves significant double-bond character (WBI = 1.59). Moreover, the new C–O bond formed between the O atom on the polyoxometalate surface and the adsorbed molecule presents a pure single bond (WBI = 0.98). Formation of this bond is accompanied by a strong weakening of the O atom bonded with nearest-neighboring Ru and W atoms (WBIs decrease from 0.76 and 0.61 in **1** to 0.43 and 0.36, respectively). The W atom compensates for the weakening of this bond by strengthening the other W–O bonds whereas the Ru atom shows a tendency to form an $O_2Ru–OCO_2$ moiety. Thus, the geometric and electronic structures of the entire polyoxometalate undergo significant changes induced by the coordination of CO_2 directed to partial reduction of Ru^{III}. It will be seen from further discussion that side-on CO_2 coordination in complex **2** leads to a lesser Ru reduction, whereas formation of amino complexes **4** (see below) favors an increase of the Ru oxidation state. Therefore, we conclude that complex **3** is probably responsible for the experimentally observed electrochemical reduction of the polyoxometalate–CO_2 system.

End-on coordination with formation of complex **2** is exothermic by only 1.13 kcal mol^{-1} at RT. Thus, replacement of the water ligand by CO_2 in the end-on mode is thermodynamically unfavorable (the calculated **1**–H_2O interaction energy is 11.44 kcal mol^{-1}, Table 2). NPA reveals small (0.12 e$^-$) $CO_2 \rightarrow$Ru charge transfer in complex **2**. Positive charging causes a small deviation of the CO_2 molecule from linearity ($\sphericalangle$O-C-O = 169.5°) and appearance of minor spin density (0.007 e$^-$) on the C atom. The C–O bonds are slightly elongated upon coordination in the end-on mode. Notably, the C–O bond directly involved in the bonding with Ru is shorter than the dangling bond (1.180 and 1.193 Å, respectively), which is probably due to polarization induced by a high positive charge on the metal atom. Nonetheless, comparison of WBIs for these bonds (1.696 and 1.930, respectively) indicates that the former bond slightly weakens whereas the latter one strengthens upon coordination.

Although amines are frequently used as hydrogen (electron, proton) donors in catalytic CO_2 reduction as noted above, the interaction of amines with CO_2 has not been considered in these reactions,[21] even though the reaction of many amines with CO_2 is well known.[22] Our computations show that the interaction between CO_2 and trimethylamine (NMe_3) is thermodynamically favorable at 0 K. At RT the interaction becomes slightly endothermic due to the entropy effect (Table 2). Triethylamine (NEt_3) is a stronger nucleophile and thus forms a more stable complex with CO_2, such that the interaction is exothermic at RT (Table 2). The NR_3 to CO_2 electron donation of about 0.01 e$^-$ results in slight bending of the CO_2 moiety, $\sphericalangle$O-C-O = 172.9° and 171.8° for R = Me and Et, respectively, and in the elongation of the C–O bonds. Notably, this elongation is not symmetric for the two C–O bonds, and the oxygen atom of the more activated bond keeps a somewhat larger negative charge. These results indicate that electron donation from the amine causes some sp^2 hybridization of the carbon atom. Indeed, conjugation of the two π orbitals in CO_2 results in its linear geometry and governs the high stability of the CO_2 molecule. The lowest unoccupied molecular orbital (LUMO) of CO_2 is strongly antibonding with respect to the C–O bonds. Thus, electron donation from the amine results in weakness of the C–O bonds whereas CO_2 bending reduces this unfavorable effect (Figure 6). Therefore, deviation from linearity could

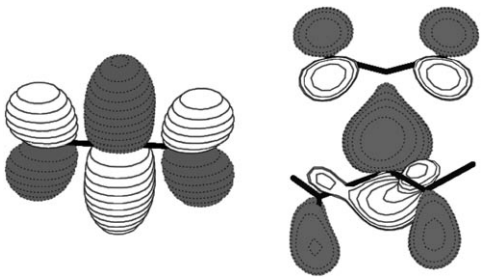

Figure 6. LUMO of free CO_2 (left) and HOMO of the CO_2–NMe_3 complex (right).

serve as a measure of CO_2 activation. The highest occupied molecular orbital (HOMO) of CO_2 rises in energy whereas the LUMO goes down upon bending, thus both the electrophilicity and nucleophilicity of CO_2 are increased.

However, the interaction between CO_2 and NR_3 in the gas phase (as well as in nonpolar solvents) is very weak with

a long (2.691 Å for R = Me and 2.654 Å for R = Et) C–N bond and WBI of 0.027 and 0.029, respectively. The end-on CO_2 coordination makes the carbon atom more prone to nucleophilic attack by the amines (Figure 7) so that the interaction of NMe_3 and NEt_3 with **2** is accompanied by an energy gain of 9.89 and 28.72 kcal mol^{-1}, respectively, at RT.[23] The C–N bond in **4-NMe$_3$** and **4-NEt$_3$** is shortened to 2.125 and 2.057 Å and the WBI increases to 0.220 and 0.291, respectively. The O-C-O angle (150.9° in **4-NMe$_3$** and 148.0° in **4-NEt$_3$**), the C–O bond elongation, and the asymmetry of the CO_2 fragment (Figure 7) are much stronger in **4** than in the CO_2–NR_3 interaction. Again, the oxygen atom involved in the bonding with Ru forms a shorter C–O bond than the other oxygen atom, whereas the WBIs (1.616 versus 1.824 for **4-NMe$_3$** and 1.583 versus 1.792 for **4-NEt$_3$**, respectively) indicate that the Ru-bound oxygen atom forms a weaker C–O bond. Although the CO_2 fragment remains almost neutral, the electron density within the fragment slightly shifts towards oxygen atoms in the presence of the amine. The NR_3 to CO_2 electron donation (0.07 (R = Me) and 0.12 e$^-$ (R = Et)) is somewhat higher in **4** than in the zwitterion.

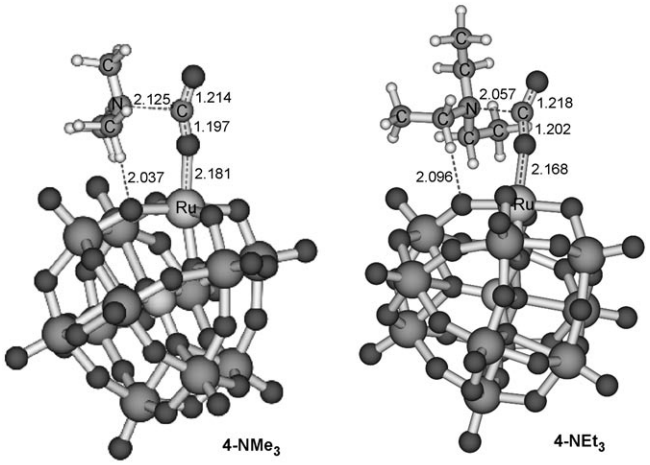

Figure 7. Optimized geometries of amine-assisted CO_2 coordination with polyoxometalate (W: large gray spheres, Si: large light gray spheres, O: medium dark gray spheres, H: small white spheres; Ru, C, and N atoms are explicitly labeled).

Most importantly, the amine to CO_2 electron donation dramatically increases the coordination ability of CO_2. Interaction of the CO_2–NR_3 adduct with **1** is exothermic by 15.39 (R = Me) and 22.53 kcal mol^{-1} (R = Et) at RT. Although the interaction causes only modest changes in the distances between the Ru and O atoms of the Keggin unit (Table 3), the electronic structure of the complex undergoes significant modification. In particular, the positive charge on the Ru atom increases from 3.76 in **1** and 3.55 in **2** to 4.11 in **4-NMe$_3$** and 4.27 in **4-NEt$_3$**. The spin density, which is highly localized on the Ru atom in all the studied Ru^{III} complexes (0.81–0.92 e$^-$), is redistributed between the polyoxometalate metal atoms in **4** and only 0.10 unpaired electron density remains on the Ru atom.

Another important feature of complex **4** is the formation of a hydrogen bond between the ᵅCH of the amines and the oxygen atom on the polyoxometalate surface. Formation of a CH···O bond was proven theoretically[24] and experimentally[25] for various compounds, particularly for quaternary amines.[26] Depending on the strength of the electron donor, the energy of the CH···O bond in complexes of quaternary amines varies from 8–10 to 20–23 kcal mol^{-1} and the attachment energies of ligands to Et_3N^+ are smaller by 2 kcal mol^{-1} than those to Me_4N^+.[26a] The length of the hydrogen bonds in the weakly bound complexes was found to be 2.59–2.70 Å.[26a] We found significantly shorter hydrogen bonds in complexes **4** (Figure 6), whereas NEt_3 forms a somewhat longer H bond than NMe_3. Although in several systems the CH···O interaction was found to shorten the C–H bond,[24a] complexes **4** show the conventional behavior, that is, the C–H bonds are slightly stretched (from 1.099 Å in NMe_3 to 1.109 Å in **4-NMe$_3$** and from 1.107 Å in NEt_3 to 1.110 Å in **4-NEt$_3$**). High positive atomic polar tensor (APT) charges on the H atoms involved in the CH···O bonding (0.176 and 0.153) as compared to those on other H atoms (from −0.149 to +0.118 and from −0.141 to +0.125 in **4-NMe$_3$** and **4-NEt$_3$**, respectively) indicate strong $C^{\delta-}$–$H^{\delta+}$ polarization upon stretching C–H vibration. Electronic structure analysis confirms the weakness of C–H bonds in these complexes (WBI_{C-H} = 0.863 and 0.854) with respect to the corresponding amines (WBI_{C-H} = 0.900 and 0.878, respectively). Notably, in spite of the stronger CH···O interaction in **4-NMe$_3$** (WBI_{H-O} = 0.026) than in **4-NEt$_3$** (WBI_{H-O} = 0.018), the secondary C–H bond remains somewhat weaker than the primary C–H bond.

Analysis of the electronic structure reveals that the HOMO in complexes **4** is localized mainly on the Ru atom. It has weakly bonding character with respect to C–O_{Ru} interaction, but it is repulsive with respect to Ru–OCO, O_2C–NR_3, and C–$O_{dangling}$ bonds (Figure 8a). On the contrary, the LUMO of these complexes is antibonding with respect to C–O_{Ru} and C–$O_{dangling}$ bonds and slightly bonding with respect to Ru–OCO and O_2C–NR_3 (Figure 8b). As frontier orbitals are usually strongly involved in photochemical processes, these results imply, in the first approximation, that photochemical excitation of complexes **4** favors breaking of the C–O_{Ru} bond and stabilization of O_2C–NR_3 and Ru–O interactions.

All in all, the electronic structure analysis shows that the polyoxometalate takes part in activation of both CO_2 and amine. The end-on CO_2 coordination favors nucleophilic attack at the carbon atom, which stabilizes the carbon sp^2 hybridization state. Formation of the O_2C–NMe_3 zwitterion, in turn, causes bending of the CO_2 molecule and enhances carbon sp^2 hybridization. Thus, the promotional effect of an amine on the activation of CO_2 by $[Ru^{III}(H_2O)SiW_{11}O_{39}]^{5-}$ may be attributed to a synergetic effect of these two interactions. Amine to CO_2 electron donation enhances the acidity of C–H bonds and results in strong hydrogen bonding with nucleophilic centers on the polyoxometalate surface.

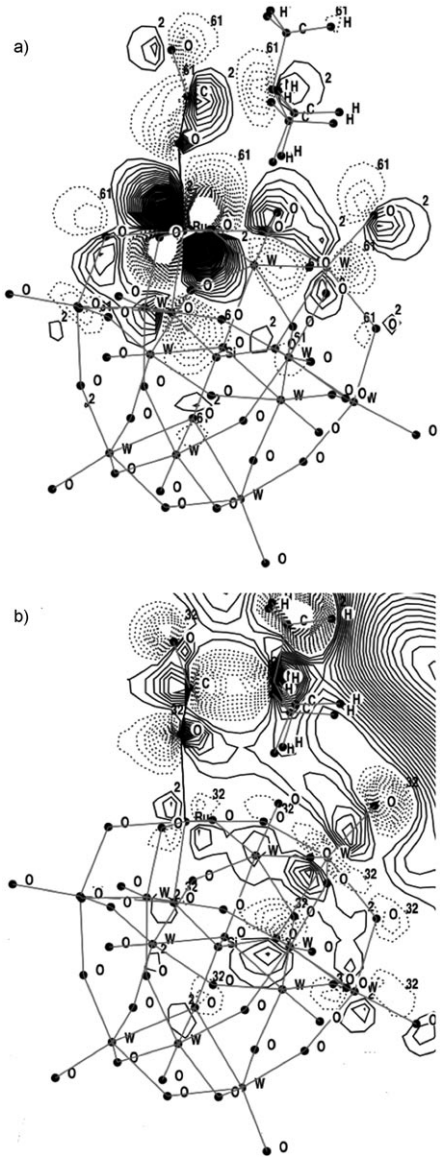

Figure 8. a) HOMO and b) LUMO of **4-NMe$_3$** calculated at the M06/PC1//PBE/PC1-DF level of theory.

Conclusion

The coordination, photochemical, and computational studies suggest the following pathway for CO_2 reduction (see Scheme 1). First, $^6Q_5[Ru^{III}(H_2O)SiW_{11}O_{39}]$ coordinates CO_2 and in the presence of a tertiary amine a $^6Q_5[Ru^{III}(CO_2–NR_3)SiW_{11}O_{39}]$ complex is formed. Formation of a CH···O bond implies that there is equilibrium between the quaternary amine and imine forms of the complex. This stage is common for all the studied hydrogen-containing amines. Indeed, imine formation is observed with Bz_3N even though there is no CO_2 reduction, and for NEt_3, NPh_3, and iPr_2EtN the amine conversion is also higher than the CO_2 conversion (Table 1). When sterically possible, particularly if Et_3N is used as hydrogen donor, the unsaturated carbon atom of aliphatic imines tends to bond to one of the O atoms of CO_2. Photoexcitation of the polyoxometalate leads to breaking of the C–O bond of CO_2 and strengthening of the C_{imine}–O bond followed by decomposition of the imine into acetaldehyde and O=C–NEt_2. Interaction of the latter with a H atom on the polyoxometalate surface results in diethylamine and release of CO. When triphenylamine is used as a reductant, the formation of a C_{imine}–O bond is sterically hampered. *N*-Phenylcarbazole is formed by subsequent dehydrogenation of two aromatic rings, which results in formation of a H_2O moiety on the polyoxometalate surface and probably is followed by dissociation of a water molecule.[27] The empty oxygen site on the polyoxometalate surface is readily occupied by the apical O atom formed as a result of CO_2 photolysis. Transformations of amines that are not accompanied by CO_2 reduction follow, probably, a similar dehydrogenation process with consequent movement of H atoms to the empty Ru center and release of hydrogen.

Further research will be directed to improving the efficiency of the photochemical system and to substituting sacrificial amines for hydrogen donors that can be regenerated.

Experimental Section

Materials: All chemicals were reagent grade and used as supplied. The lacunary $K_8[SiW_{11}O_{39}]\cdot 13H_2O$ polyoxometalate was prepared by a known literature method.[28] The ruthenium(III)-substituted polyoxometalate $K_5[Ru^{III}(H_2O)SiW_{11}O_{39}]\cdot 10H_2O$ was prepared by following the literature method and analyzed by elemental analysis, UV/Vis and IR spectroscopy, and cyclic voltammetry.[12] The tetrahexylammonium salt of $[Ru^{III}(H_2O)SiW_{11}O_{39}]^{5-}$ was prepared by a modification of the method introduced by Katsoulis and Pope.[14] Thus, an aqueous solution of $K_5[Ru^{III}(H_2O)SiW_{11}O_{39}]\cdot 10H_2O$ (10 mM) was shaken with an equal volume of a solution of tetrahexylammonium bromide (50 mM) in toluene. After the two phases had been allowed to settle for 10 min, the organic phase was separated and dried over Na_2SO_4 and the solvent removed by vacuum. CHN and thermogravimetric elemental analysis revealed a formula consistent with $[(C_6H_{13})_4N]_{4.9}K_{0.1}[Ru^{III}(H_2O)SiW_{11}O_{39}]$. CO_2 (>99.99% purity) was purchased from Gordon Gas, and $^{13}CO_2$ (99% enrichment) was purchased from Cambridge Isotope Laboratories.

Methods: GC and GC–MS were carried out on HP 6890 (flame ionization detector and thermal conductivity detector (TCD)) and HP 5973 (MS detector) instruments equipped with a 30 m column (Restek 5MS, 0.32 mm internal diameter) with a 5% phenylmethylsilicone coating (0.25 μm) and helium as carrier gas. The gaseous reaction products including CO were analyzed by GC–TCD with a Carbonplot capillary column (J&W Scientific). NMR spectra were measured on a Bruker Avance 500 MHz instrument. ^{13}C NMR spectra were recorded under short relaxation time and short delay time conditions. Cyclic voltammetry was performed on a model 600C apparatus (HCH Instruments) at ambient temperature. A glassy-carbon working electrode (diameter 3 mm), a platinum-wire counter electrode, and an Ag/Ag^+ reference electrode were used. UV/Vis spectra were recorded by using an HP 8453 diode-array spectrophotometer. Electron spin resonance spectra were recorded with a Bruker Elexys 500 instrument. A solution of $^6Q_5[Ru^{III}SiW_{11}O_{39}]$ (10 mM) in toluene saturated with CO_2 was prepared at 125 K, and spectra were recorded under the following conditions: microwave frequency, 9.33 GHz; microwave power, 25 mW; field modulation, 100 mG; receiver gain, 60; time constant, 1.31 s.

Photocatalytic reactions: In a typical reaction, toluene solution (3 mL) containing the polyoxometalate complex and triethylamine in a 20 mL quartz pressure tube was saturated with CO_2 by bubbling through the solution for 10 min and then the pressure was raised to 2 bar. The solution

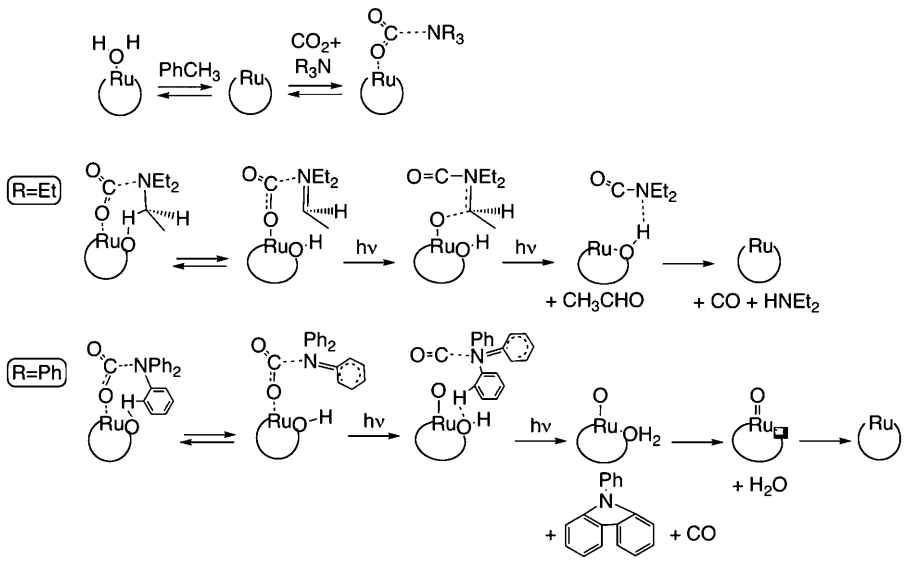

Scheme 1. Proposed mechanism for the photoreduction of CO_2 with tertiary amines catalyzed by $^6Q_5[Ru^{III}(H_2O)SiW_{11}O_{39}]$.

was irradiated with an LS 150 xenon arc lamp source. The quantum yield is defined per two absorbed photons because the formation of one molecule of CO requires two photons, as shown in Scheme 1. The irradiation power measured in front of the reaction cuvette with an Ophir thermal head power meter was 50 mW. Assuming that all light entering the reaction solution was absorbed, the estimated quantum yield for CO formation was 0.02.

Computational methods: All computations were performed with the Gaussian 03 package.[29] Initially, geometry optimizations were performed at the DFT[30] level by using the nonempirical generalized gradient approximation (GGA) density functional PBE[31] (also known as PBEPBE) combined with the SDD basis set, which is a combination of the Huzinaga–Dunning double-ζ basis set[32] on lighter elements with the Stuttgart–Dresden basis set–RECP combination[33] on transition metals. Additional PBE and M06L[34] geometry optimizations were carried out with a larger basis set PC1, which for transition metals consists of SDD with an added *f* function with an exponent calculated as a geometric mean of the 2*f* exponents given in ref. [35] and of Jensen's "polarization-consistent" pc-1 basis set[36] on the remaining elements. The density-fitting (DF)[37] approach for treatment of the two-electron (Coulomb) integrals was applied in all the optimization calculations. The DF approach implemented in Gaussian 03 provides significant performance gains for pure DFT calculations without a significant degradation in the accuracy of predicted structures, relative energies, and molecular properties. The accuracy of the computational methods in prediction of the geometry of the complexes was validated by calculation of the $[Ru^{III}(H_2O)SiW_{11}O_{39}]^{5-}$ complex **1-H$_2$O** (Figure 5), for which the experimental geometry of its Cs salt is known[12] (see Table 3 and the Supporting Information). Unfortunately, due to the two types of disorder found for the $Cs_5[Ru^{III}(H_2O)SiW_{11}O_{39}]$ crystal structure, the Ru center could not be distinguished from the W atoms. The M06L/PC1-DF approach provided the best agreement with the experimental data. However, we faced significant convergence difficulties when using this functional. Thus, the PBE/PC1-DF combination was chosen for optimization of complex geometries. Differences between the bond lengths optimized with these two approaches did not exceed 0.037 Å. Optimized structures were characterized as minima by calculating harmonic vibrational frequencies at the PBE/SDD-DF and PBE/PC1-DF levels of theory. All calculations were performed on the lowest-spin (doublet) potential energy surface. For interpretative purposes, atomic partial charges and WBIs[38] were obtained by means of NPA[39] at the M06/PC1//PBE/PC1-DF level of theory.

Acknowledgements

This research was supported by the Divadol Foundation, the Israel Science Foundation, and the Helen and Martin Kimmel Center for Molecular Design. R.N. is the Rebecca and Israel Sieff Professor of Chemistry. J.M.L.M. holds the Baroness Thatcher Professorial Chair of Chemistry. A.M.K. and I.E. acknowledge the financial support of the Center for Adsorption in Science, Ministry of Immigrant Absorption, State of Israel.

[1] N. S. Lewis, D. G. Nocera, *Proc. Natl. Acad. Sci. USA* **2006**, *103*, 15729.

[2] a) L. Hammarstrom, *Curr. Opin. Chem. Biol.* **2003**, *7*, 666; b) *Artificial Photosynthesis: From Basic Biology to Industrial Application* (Eds.: A. F. Collings, C. Critchley), Wiley-VCH, Weinheim, **2005**, p. 313; c) S. Fukuzumi, *Bull. Chem. Soc. Jpn.* **2006**, *79*, 177; d) M. H. V. Huynh, D. M. Dattelbaum, T. J. Meyer, *Coord. Chem. Rev.* **2005**, *249*, 457; e) K. Szacilowski, W. Macyk, A. Drzewiecka-Matuszek, M. Brindell, G. Stochel, *Chem. Rev.* **2005**, *105*, 2647; f) E. Fujita, B. S. Brunschwig, *Electron Transfer Chem.* **2001**, *4*, 88; g) L. Sun, L. Hammarstrom, B. Akermark, S. Styring, *Chem. Soc. Rev.* **2001**, *30*, 36.

[3] a) I. Omae, *Catal. Today* **2006**, *115*, 33; b) M. Aresta in *Activation of Small Molecules* (Ed.: W. B. Tolman), Wiley-VCH, Weinheim, **2006**, p. 1.

[4] a) M. T. Whited, R. H. Grubbs, *J. Am. Chem. Soc.* **2008**, *130*, 5874; b) C. C. Lu, C. T. Sauoma, M. W. Day, J. C. Peters, *J. Am. Chem. Soc.* **2007**, *129*, 4; c) D. S. Laitar, P. Muller, J. P. Sadighi, *J. Am. Chem. Soc.* **2005**, *127*, 17196.

[5] a) W. Lin, H. Han, H. Frei, *J. Phys. Chem. B* **2004**, *108*, 18269; b) M. Anpo, M. Takeuchi, *J. Catal.* **2003**, *216*, 505.

[6] J. Grodkowski, P. Neta, *J. Phys. Chem. A* **2000**, *104*, 4475.

[7] E. Fujita, B. S. Brunschwig, T. Ogata, S. Yanagita, *Coord. Chem. Rev.* **1994**, *132*, 195.

[8] J. Hawecker, J.-M. Lehn, R. Ziessel, *J. Chem. Soc. Chem. Commun.* **1985**, 56.

[9] Z.-Y. Bian, K. Sumi, M. Furue, S. Sato, K. Koike, O. Ishitani, *Inorg. Chem.* **2008**, *47*, 10801.

[10] C. L. Hill, D. A. Bouchard, *J. Am. Chem. Soc.* **1985**, *107*, 5148.

[11] S. H. Szczepankiewicz, C. M. Ippolito, B. P. Santora, T. J. Van de Ven, G. A. Ippolito, L. Fronckowiak, F. Wiatrowski, T. Power, M. Kozik, *Inorg. Chem.* **1998**, *37*, 4344.

[12] a) Y. V. Geletii, B. Botar, P. Koegerler, D. A. Hillesheim, D. G. Musaev, C. L. Hill, *Angew. Chem.* **2008**, *120*, 3960; *Angew. Chem. Int. Ed.* **2008**, *47*, 3896; b) A. Sartorel, M. Carraro, G. Scorrano, R. De Zorzi, S. Geremia, N. D. McDaniel, S. Bernhard, M. Bonchio, *J. Am. Chem. Soc.* **2008**, *130*, 5006; c) A. R. Howells, A. Sankarraj, C. J. Shannon, *J. Am. Chem. Soc.* **2004**, *126*, 12258.

[13] M. Sadakane, D. Tsukuma, M. H. Dickman, B. Bassil, U. Kortz, M. Higashijima, W. Ueda, *Dalton Trans.* **2006**, 4271.

[14] D. E. Katsoulis, M. T. Pope, *J. Am. Chem. Soc.* **1984**, *106*, 2737.

[15] R. Neumann, C. Abu-Gnim, *J. Am. Chem. Soc.* **1990**, *112*, 6025.

[16] D. A. Bardwell, D. Black, J. C. Jeffery, E. Schatz, M. D. Ward, *J. Chem. Soc. Dalton Trans.* **1993**, 2321.

[17] M. Sadakane, M. Hijashijima, *Dalton Trans.* **2003**, 659.

[18] a) T. Yamase, *Catal. Surv. Asia* **2003**, *7*, 203; b) M. Fagnoni, D. Dondi, D. Ravelli, A. Albini, *Chem. Rev.* **2007**, *107*, 2725; c) C. L. Hill, C. M. Prosser-McCartha, *Coord. Chem. Rev.* **1995**, *143*, 407.

[19] M. Sadakane, Y. Iimuro, D. Tsukuma, B. S. Bassil, M. H. Dickman, U. Kortz, Y. Zhang, S. Ye, W. Ueda, *Dalton Trans.* **2008**, 6692.
[20] Y. Zhao, D. G. Truhlar, *Theor. Chem. Acc.* **2008**, *120*, 215.
[21] R. D. Richardson, B. K. Carpenter, *J. Am. Chem. Soc.* **2008**, *130*, 3169.
[22] M. Aresta, A. Dibenedetto, *Dalton Trans.* **2007**, 2975.
[23] Even though the side-on coordinated complex **3** is more favorable than the end-on complex **2**, the reaction with amines to form **4** is considered with **2** because **3** has no free electrophilic centers capable of forming a bond with an amine. It also should be noted that **4** can also be formed by the formation of CO_2–NR_3 followed by its reaction with **1** ($\Delta G_{298} = -22.53$ kcal mol^{-1} for **4-NEt$_3$**).
[24] a) Y. Gu, T. Kar, S. Scheiner, *J. Am. Chem. Soc.* **1999**, *121*, 9411; b) R. Vargas, J. Garza, D. A. Dixon, B. P. Hay, *J. Am. Chem. Soc.* **2000**, *122*, 4750; c) J. Schwöbel, R.-U. Ebert, R. Kühne, G. Schürmann, *J. Comput. Chem.* **2009**, *30*, 1454.
[25] R. Taylor, O. Kennard, *J. Am. Chem. Soc.* **1982**, *104*, 5063.
[26] a) M. Meot-Ner, C. A. Deakyne, *J. Am. Chem. Soc.* **1985**, *107*, 469; b) A. N. Chekhlov, *Russ. Chem. Bull.* **1990**, *99*, 2505.
[27] Although the proposed mechanism with NPh_3 as related to release of a water molecule is speculative, preliminary and ongoing computational research on the reaction of protons on polyoxometalate surfaces appears to support such an idea.
[28] R. Contant, *Inorg. Synth.* **1990**, *27*, 104.
[29] Gaussian 03, Revision E.01, M. J. Frisch, G. W. Trucks, H. B. Schlegel, G. E. Scuseria, M. A. Robb, J. R. Cheeseman, J. A. Montgomery, Jr., T. Vreven, K. N. Kudin, J. C. Burant, J. M. Millam, S. S. Iyengar, J. Tomasi, V. Barone, B. Mennucci, M. Cossi, G. Scalmani, N. Rega, G. A. Petersson, H. Nakatsuji, M. Hada, M. Ehara, K. Toyota, R. Fukuda, J. Hasegawa, M. Ishida, T. Nakajima, Y. Honda, O. Kitao, H. Nakai, M. Klene, X. Li, J. E. Knox, H. P. Hratchian, J. B. Cross, V. Bakken, C. Adamo, J. Jaramillo, R. Gomperts, R. E. Stratmann, O. Yazyev, A. J. Austin, R. Cammi, C. Pomelli, J. W. Ochterski, P. Y. Ayala, K. Morokuma, G. A. Voth, P. Salvador, J. J. Dannenberg, V. G. Zakrzewski, S. Dapprich, A. D. Daniels, M. C. Strain, O. Farkas, D. K. Malick, A. D. Rabuck, K. Raghavachari, J. B. Foresman, J. V. Ortiz, Q. Cui, A. G. Baboul, S. Clifford, J. Cioslowski, B. B. Stefanov, G. Liu, A. Liashenko, P. Piskorz, I. Komaromi, R. L. Martin, D. J. Fox, T. Keith, M. A. Al-Laham, C. Y. Peng, A. Nanayakkara, M. Challacombe, P. M. W. Gill, B. Johnson, W. Chen, M. W. Wong, C. Gonzalez, J. A. Pople, Gaussian Inc., Wallingford CT, **2004**.
[30] a) W. Kohn, L. J. Sham, *Phys. Rev. A* **1965**, *140*, 1133; b) R. G. Parr, W. Yang, *Density Functional Theory of Atoms and Molecules*, Oxford University Press, New York, **1970**, p. 230.
[31] a) J. P. Perdew, K. Burke, M. Ernzerhof, *Phys. Rev. Lett.* **1996**, *77*, 3865; b) J. P. Perdew, K. Burke, M. Ernzerhof, *Phys. Rev. Lett.* **1997**, *78*, 1396.
[32] T. H. Dunning, Jr., P. J. Hay, *Modern Theoretical Chemistry, Vol. 3*, Plenum Press, New York, **1976**, p. 1.
[33] M. Dolg in *Modern Methods and Algorithms of Quantum Chemistry, Vol. 1*, John von Neumann Institute for Computing, Jülich, **2000**, p. 479.
[34] Y. Zhao, D. G. Truhlar, *J. Chem. Phys.* **1996**, *104–105*, 194101.
[35] J. M. L. Martin, A. Sundermann, *J. Chem. Phys.* **2001**, *114*, 3408.
[36] F. Jensen, *J. Chem. Phys.* **2002**, *116*, 7372.
[37] a) B. I. Dunlap, *J. Chem. Phys.* **1983**, *78*, 3140; b) B. I. Dunlap, *J. Mol. Struct.* **2000**, *529*, 37; c) A. B. Nadykto, H. Dua, F. Yu, *Vib. Spectrosc.* **2007**, *44*, 286.
[38] K. B. Wiberg, *Tetrahedron* **1968**, *24*, 1083.
[39] A. E. Reed, L. A. Curtiss, F. Weinhold, *Chem. Rev.* **1988**, *88*, 899.

Received: June 18, 2009
Revised: October 13, 2009
Published online: December 9, 2009

